Model of Thin-Film Microstrip Line for Circuit Design

Frank Schnieder and Wolfgang Heinrich, *Senior Member, IEEE*

***Abstract*—An equivalent-circuit model for the thin-film microstrip line (TFMSL) is presented in this paper. Its elements are calculated using closed-form expressions and, thus, this model can easily be implemented in common circuit design tools. For typical TFMSL dimensions, it holds from dc up to the submillimeter-wave frequency range. The model is validated by comparison to electromagnetic full-wave simulation data. Typical errors of phase constant and characteristic impedance are below 2% and 3%, respectively. Regarding attenuation, deviations below 8% are found.**

***Index Terms*—Equivalent-circuit model, losses, microstrip, multichip modules, thin-film circuits.**

I. Introduction

THIN-FILM microstrip lines (TFMSLs) find more and more applications, especially in Si-based monolithic microwave integrated circuits (MMICs) [1], [2] and as transmission lines in multichip modules (MCMs) [3]. They are miniaturized microstrip lines (MSLs) located on top of the substrate. One special advantage is that the ground metallization of the TFMSL shields the line from the substrate effects. Therefore, e.g., low-resistivity silicon substrates can be used without deteriorating microwave performance. Since high-quality polymers, e.g., polyimide or Benzocyclobutene (BCB), are available as dielectric layers, attenuation of such TFMSLs is comparable with coplanar waveguides (CPWs) in GaAs MMICs. Since transversal dimensions can be scaled down, miniaturized TFMSLs show excellent low-dispersive properties and can be used up to the submillimeter-wave range [4].

However, for a broad utilization of TFMSLs, one needs simplified models for circuit design. For conventional MSLs, a variety of closed-form models are available in the literature and as software packages [5], [6]. However, since dimensions of the TFMSL and conventional MSL differ considerably, applying the common MSL models to TFMSLs yields significant errors. For conventional MSLs, the dielectric is identical with the circuit substrate. Height and width of the signal conductor are in the range of hundreds of micrometers (in MMICs, the substrate thickness varies from 254 to 100 μm). For TFMSLs, on the other hand (see Fig. 1), these values are around 10 μm and, thus, in the order of magnitude of the metallization thickness. These differences in geometrical dimensions cause discrepancies in the electrical behavior. Small dimensions increase conductor loss. Due to the relative large t/h_s ratio, finite metal conductivity and internal inductance have to be taken into account. Therefore, in the TFMSL case, phase constant and characteristic impedance deviate considerably from the lossless case and show the typical increase toward lower frequencies known from CPWs [7]. On the other hand, because TFMSL line dimensions remain small compared to wavelength, the quasi-TEM approximation holds well and dispersion due to nonquasi-TEM behavior plays a minor role.

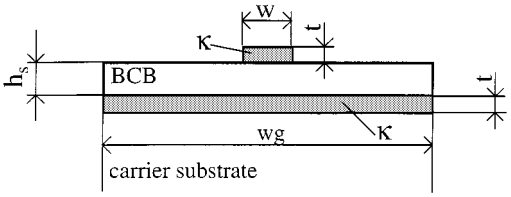

Fig. 1. TFMSL: cross section with dimensions and material parameters (for the carrier substrate, 380 μm-thick silicon with $\varepsilon_r = 11.67$, $\kappa = 20$ S/m is assumed).

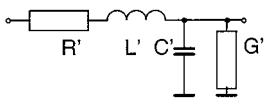

Fig. 2. Distributed equivalent-circuit model of the TFMSL.

Due to the quasi-TEM behavior, a distributed equivalent-circuit model can be used for describing the TFMSL with good accuracy. The circuit is shown in Fig. 2. The elements of the equivalent circuit are related to different physical effects and can be determined separately. As a consequence of its simple structure, conversion between circuit elements and complex propagation quantities has a one-to-one correspondence.

As well known from quasi-TEM theory, capacitance and conductance are related to the electrostatic case and, thus, constant with frequency (except for non-TEM contributions), whereas inductance and resistance are determined by magneto-quasi-statics. Therefore, the latter quantities vary with the longitudinal current distribution, which is frequency dependent due to the skin effect.

The procedure in determining the equivalent-circuit elements R', L', C', G' was as follows. First, the element values were extracted from the results of electromagnetic simulations by a full-wave mode-matching method [7] that rigorously takes into account conductor and dielectric losses. This provided both quantitative reference values and a physical understanding. Based on these results, closed-form approximations were derived for R', L', C', and G' utilizing the numerous approaches

Manuscript received July 16, 1999. This work was supported by the Deutsche Forschungsgemeinschaft under Contract He 1676/10.

The authors are with the Ferdinand-Braun-Institut für Höchstfrequenztechnik, D-12489 Berlin, Germany.

Publisher Item Identifier S 0018-9480(01)00021-7.

for conventional MSLs available in the literature. Extending these descriptions, an efficient model for the TFMSL was established, which is suitable for practical circuit design. Accuracy of the new model is established by comparing the line parameters to numerical full-wave simulation results.

The paper is organized as follows. Sections II and III describe derivation of the formulas for the equivalent-circuit elements, i.e., C', G', and L', R', respectively. In Section IV, accuracy and limitations of the model are discussed and Section V presents conclusions.

II. Capacitance C' and Conductance G'

Checking accuracy of the conventional microstrip approximations of C' for the TFMSL structure, one finds that the formulas available in the literature hold with good accuracy and do not need major modifications. Hence, the issue of this section is selecting suitable expressions rather than developing a new approach. Nevertheless, for the sake of clarity, the formulas are briefly described below in order to provide the reader with the complete set of information and to avoid doubts as to definitions of parameters, etc. This is considered to be essential for the new model being useful for computer-aided design (CAD) implementation.

Generally, the capacitance C' of quasi-TEM lines can be calculated by means of a Schwartz–Christoffel conformal mapping procedure. However, in contrast to the CPW case, this method is difficult to apply to the microstrip geometry because the interface between the dielectric layer and air does not coincide with an electrical field line. In the literature, several approximate solutions for that problem are available [5], [6]. Mostly, the formulas of Hammerstad and Jensen [8] are used because they promise the highest accuracy for a broad range of applications.

In the lossless case with $t = 0$ and $\varepsilon_r = 1$ (for parameter definition, see Fig. 1), i.e., for a line structure with zero metal thickness and without substrate, the formula for characteristic impedance reads [5, p. 156]

$$Z_{L0} = \frac{\eta_0}{2\pi} \cdot \ln\left\{ \frac{F_1 \cdot h_s}{w} + \sqrt{1 + \left(\frac{2 \cdot h_s}{w}\right)^2} \right\} \tag{1}$$

with

$$F_1 = 6 + (2\pi - 6) \cdot \exp\left\{ -\left(30.666 \cdot \frac{h_s}{w}\right)^{0.7528} \right\}$$

and

$$\eta_0 = \sqrt{\frac{\mu_0}{\varepsilon_0}}.$$

Including a dielectric substrate, i.e., for $\varepsilon_r > 1$, the effective relative dielectric constant of the MSL is

$$\varepsilon_{r,\,\mathrm{eff},\,0} = \frac{\varepsilon_r + 1}{2} + \frac{\varepsilon_r - 1}{2} \cdot \left(1 + \frac{10 \cdot h_s}{w}\right)^{-a \cdot b} \tag{2}$$

with

$$a = 1 + \frac{1}{49} \cdot \ln\left\{ \frac{\left(\frac{w}{h_s}\right)^4 + \left(\frac{w}{52 \cdot h_s}\right)^2}{\left(\frac{w}{h_s}\right)^4 + 0.432} \right\} + \frac{1}{18.7} \cdot \ln\left\{ 1 + \left(\frac{w}{18.1 \cdot h_s}\right)^3 \right\}$$

and

$$b = 0.564 \cdot \left(\frac{\varepsilon_r - 0.9}{\varepsilon_r + 3}\right)^{0.053}.$$

This holds for conventional MSLs. Regarding TFMSLs, the finite thickness of the signal conductor has to be taken into account, which usually is included by an effective increase in conductor width. When using (1) and (2) for $t > 0$, the width w of the line is replaced by an equivalent conductor width w_{eq}. Again, the two cases with and without dielectric have to be distinguished. Approximating the MSL characteristic impedance without line substrate, i.e., $\varepsilon_r = 1$, $t > 0$, $w_{\mathrm{eq}0}$ [according to (3)] is to be used [5, p. 165], whereas for $\varepsilon_r > 1$, $w_{\mathrm{eq}Z}$, as shown in (4), has to be applied as follows:

$$w_{\mathrm{eq}0} = w + \frac{t}{\pi} \cdot \ln\left\{ 1 + \frac{4 \cdot \exp(1)}{\frac{t}{h} \cdot \coth^2\left(\sqrt{6.517 \cdot \frac{w}{h_s}}\right)} \right\} \tag{3}$$

$$w_{\mathrm{eq}Z} = w + \frac{w_{\mathrm{eq}0} - w}{2} \cdot \left(1 + \frac{1}{\cosh\left(\sqrt{\varepsilon_r - 1}\right)}\right). \tag{4}$$

Based on (1)–(4), characteristic impedance and effective relative dielectric constant of the lossless microstrip in the case $\varepsilon_r > 1$ and $t > 0$ can be described by

$$Z_L = \frac{Z_{L0}(w_{\mathrm{eq}Z})}{\sqrt{\varepsilon_{r,\,\mathrm{eff},\,0}(w_{\mathrm{eq}Z})}}, \tag{5}$$

$$\varepsilon_{r,\,\mathrm{eff}} = \varepsilon_{r,\,\mathrm{eff},\,0}(w_{\mathrm{eq}Z}) \cdot \left[\frac{Z_{L0}(w_{\mathrm{eq}0})}{Z_{L0}(w_{\mathrm{eq}Z})}\right]^2. \tag{6}$$

These quantities can be expressed in terms of the line elements: The capacitance per unit length of the line without dielectric substrate ($\varepsilon_r = 1$) is given by the characteristic impedance Z_{L0} and free-space light velocity c_0 [6, p. 380]

$$C'_a = \frac{1}{c_0 \cdot Z_{L0}(w_{\mathrm{eq}0})}. \tag{7}$$

Accordingly, the capacitance per unit length of the line with dielectric substrate ($\varepsilon_r > 1$) is

$$C' = \varepsilon_{r,\,\mathrm{eff}} \cdot C'_a. \tag{8}$$

The conductance per unit length G' accounts for the dielectric loss of the substrate, described by the dielectric-loss tangent $\tan\delta_\varepsilon$. For the calculation of G', only the part of the capacitance

that is filled with dielectric substrate has to be considered. Thus, one has [5, p. 126]

$$C'_{\varepsilon} = \frac{\varepsilon_{r,\,\mathrm{eff}} - 1}{\varepsilon_r - 1} \cdot \varepsilon_r \cdot C'_a \tag{9}$$

which results in a conductance per unit length of

$$G' = \omega \cdot C'_{\varepsilon} \cdot \tan(\delta_{\varepsilon}). \tag{10}$$

The capacitance and conductance values calculated in this way agree very well with values from numerical full-wave simulations (error below 1%). As expected from quasi-TEM theory, due to its electrostatic origin, C' and, thus, G'/ω are frequency independent up to the beginning of the non-TEM dispersion (well beyond 100 GHz for typical TFMSLs).

III. Resistnace R' and Inductance L'

In contrast to the capacitance, line resistance R' and inductance L' exhibit a considerable frequency dependence. This behavior can be explained by the change of current-density distribution in the nonideal conductors, which is due to the varying current penetration into the conductors when increasing the frequency from dc to the skin-effect range. The frequency dependence of R' and L' can be subdivided into the following three ranges (see [7]).

1) At low frequencies near dc (all conductor dimensions are small compared with skin depth δ), the current density is homogeneous over all conductor cross sections.
2) In the skin-effect range (all conductor dimensions are large compared with skin depth δ), the current flows only in a shallow area at the conductor surface.
3) Between the two aforementioned regions, there is a transition range. Due to the great differences in line dimensions (metallization thickness about 1 μm, ground conductor width well beyond 10 μm), this frequency range may be widely expanded. For these frequencies, some dimensions are larger than δ, others are smaller. Therefore, a simple approximation of the physical behavior as in the dc or skin-effect region is not possible.

For R' and L', we found significant deviations between the conventional microstrip approximations and the actual values, particularly in the intermediate frequency range. Accordingly, modified formulas had to be developed, which are presented below. We start from the dc and skin-effect limits (Sections III-B and III-A, respectively) and then derive an approximate formula for the entire frequency range in Section III-C.

A. Skin-Effect Limit

In the skin-effect range, several approximations for the line resistance R' are available in the literature (e.g., [5], [6], [9]). We choose the formulas by Gupta [6, p. 108] and use them to describe the resistance (the subscript se denotes the skin-effect range)

$$R'_{se} = 2 \cdot Z_L \cdot \alpha_c(f) \tag{11}$$

$$\alpha_c(f) = 0.1589 \cdot A \cdot \frac{R_S(f)}{h_s \cdot Z_L} \cdot \frac{32 - \left(\frac{w_{\mathrm{eq}0}}{h_s}\right)^2}{32 + \left(\frac{w_{\mathrm{eq}0}}{h_s}\right)^2}$$

for

$$\frac{w}{h_s} \le 1$$

and

$$\alpha_c(f) = 7.0229 \cdot 10^{-6} \cdot A \cdot \frac{R_S(f) \cdot Z_L \cdot \cdot \varepsilon_{r,\,\mathrm{eff}}}{h_s} \cdot \left[\frac{w_{\mathrm{eq}0}}{h_s} + \frac{0.667 \cdot \frac{w_{\mathrm{eq}0}}{h_s}}{\frac{w_{\mathrm{eq}0}}{h_s} + 1.444}\right]$$

for

$$\frac{w}{h_s} \ge 1$$

with Z_L according to (5), $\varepsilon_{r,\,\mathrm{eff}}$ according to (6), $w_{\mathrm{eq}0}$ according to (3), and

$$A = 1 + \frac{h_s}{w_{\mathrm{eq}0}} \cdot \left[1 + \frac{1.25}{\pi} \cdot \ln\left(\frac{2 \cdot h_s}{t}\right)\right]$$

$$R_S(f) = \sqrt{\frac{\pi \cdot f \cdot \mu_0}{\kappa}}.$$

The inductance per unit length L' can be subdivided into an external and internal part. In the skin-effect range, the external inductance L'_a covering the magnetic field outside of the conductors is almost identical with the value in the lossless case and, hence, frequency independent. One has

$$L'_a = \frac{1}{c_0^2 \cdot C'_a} \tag{12}$$

with C'_a according to (7). Under skin-effect conditions, the internal inductance L'_i, describing the magnetic field inside the conductors, is related to the resistance by (13) as follows:

$$L'_i(f) = \frac{R'_{se}(f)}{\omega}. \tag{13}$$

Thus, the total inductance per unit length in the skin-effect range is

$$L'_{se} = L'_a + L'_i \tag{14}$$

with the subscript se denoting the skin-effect range.

B. DC Limit

The line resistance in the dc range R'_{DC} consists of two parts, that of the signal and that of the ground conductor, denoted by the indexes w and g, respectively,

$$R'_{\mathrm{DC}} = R'_{\mathrm{DC},\,w} + R'_{\mathrm{DC},\,g} \tag{15}$$

with

$$R'_{\mathrm{DC},\,w} = \frac{1}{\kappa \cdot w \cdot t}$$

and

$$R'_{\mathrm{DC},\,g} = \frac{1}{\kappa \cdot wg \cdot t}.$$

Determining the inductance is more difficult. However, since we have a homogeneous current distribution in the dc range, the total inductance may be derived analytically. Djordjevic and Sarkar provide a closed-form expression [9] as follows:

$$L'_{\mathrm{DC}} = \frac{-\mu_0}{2 \cdot \pi \cdot t^2} \cdot \left[\frac{1}{w^2} \cdot K_s(w,\, t) - \frac{2}{w \cdot wg} \cdot K_m(w,\, t,\, wg,\, t,\, h_s + t) + \frac{1}{wg^2} \cdot K_s(wg,\, t) \right] \tag{16}$$

with

$$K_s(a,\, b) = \mathrm{Re}\Big\{ 4 \cdot \big[K4(a) + K4(jb)\big] - 2 \cdot \big[K4(a + jb) + K4(a - jb)\big] \Big\} + \frac{1}{3} \cdot \pi \cdot a \cdot b^3$$

$$K_m(a,\, b,\, c,\, d,\, h) = \mathrm{Re}\left\{ -K4(z1 + z2 - z3 - z4 - jh) \cdot \Big|_{z1=-(a/2)}^{(a/2)} \Big|_{z2=-j(b/2)}^{j(b/2)} \Big|_{z3=-(c/2)}^{(c/2)} \Big|_{z4=-j(d/2)}^{j(d/2)} \right\}$$

$$K4(z) = \frac{z^4}{24} \left[\ln(z) - \frac{25}{12} \right]$$

where z is a complex number. K_m is the solution of a definite fourfold integral. Inserting all the combinations of the integration limits K_m results in a sum of 16 terms of the function $K4$.

C. Resulting Quasi-Static Formulas for the Entire Frequency Range

As shown in the previous sections, R' and L' can be calculated in closed form on a physical basis both in the dc and skin-effect ranges. In the transition region, however, the situation is more complicated and simplifying assumptions cannot be applied. Hence, we start from the known dc and skin-effect limit, as given above, and describe the intermediate-frequency range by purely numerical formulas fitted to the full-wave simulation data [7]. Djordjevic and Sarkar suggest the following

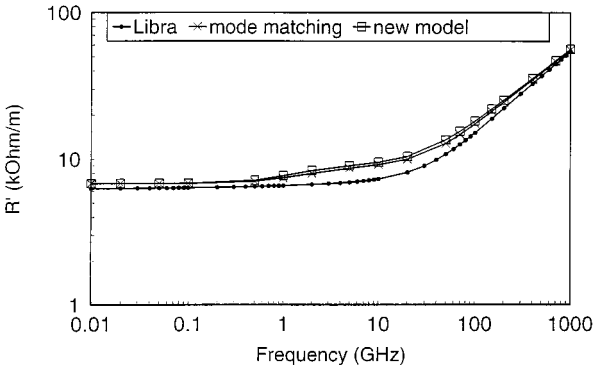

Fig. 3. Resistance per unit length R' as a function of frequency: comparison of new model with results of full-wave simulations (mode matching [7]) and Libra (TFMSL according to Fig. 1 with $w = 8\ \mu$m, $h_s = 1.7\ \mu$m, $t = 0.8\ \mu$m, $wg = 88\ \mu$m, conductivity of the metallization $\kappa = 2.5 \cdot 10^7$ S/m, BCB with $\varepsilon_r = 2.7$ and $\tan\delta_\varepsilon = 0.015$).

approximations for R' and L', as shown in (17) at the bottom of this page, and as follows in (18) [9]:

$$L'(f) = L'_a + \frac{L'_i(f_{se})}{1 + \sqrt{\dfrac{f}{f_{se}}}} + \frac{L'_{\mathrm{DC}} - L'_a - L'_i(f_{se})}{\sqrt{1 + \left(\dfrac{f}{f_0}\right)^2}}. \tag{18}$$

In these equations, f_0 and f_{se} denote the frequency boundaries between the dc and intermediate ranges and between the intermediate and skin-effect ranges, respectively. They are approximated by (19) and (20) [9] as follows:

$$f_0 = \frac{2 \cdot R'_{\mathrm{DC},\,w} \cdot R'_{\mathrm{DC},\,g}}{\mu_0 \cdot \left(R'_{\mathrm{DC},\,w} + R'_{\mathrm{DC},\,g}\right)} \tag{19}$$

$$f_{se} = \frac{1.6 + \dfrac{10 \cdot \dfrac{t}{w}}{1 + \dfrac{w}{h_s}}}{\pi \cdot \mu_0 \cdot \kappa \cdot t^2}. \tag{20}$$

Note that we use (11) and (5) for R'_{se} and Z_L, which are different from those used in the original Djordjevic and Sarkar paper.

In Figs. 3 and 4, typical curves of R' and L' as a function of frequency are plotted comparing R' and L' from our model with the full-wave simulations. Also, results of the microstrip model used in the commercial microwave circuit simulation software

$$R'(f) = R'_{\mathrm{DC}} + \frac{R'_{se}(f_{se}) \cdot \dfrac{\sqrt{\dfrac{f}{f_{se}}} + \sqrt{1 + \left(\dfrac{f}{f_{se}}\right)^2}}{1 + \sqrt{\dfrac{f}{f_{se}}}} - \dfrac{R'_{se}(f_{se}) - R'_{\mathrm{DC}}}{\sqrt{1 + \left(\dfrac{f}{f_0}\right)^2}} - R'_{\mathrm{DC}}}{1 + \dfrac{0.2}{1 + \dfrac{w}{h_s}} \cdot \ln\left(1 + \dfrac{f_{se}}{f}\right)} \tag{17}$$

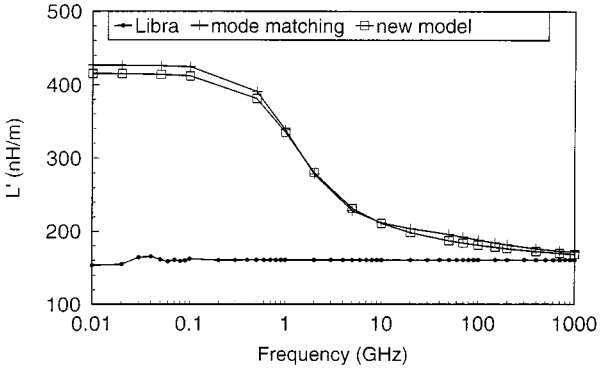

Fig. 4. Inductance per unit length L' as a function of frequency (other data as in Fig. 3).

LIBRA and ADS of HP-EEsof are included (LIBRA and ADS give identical results). It can be seen that the LIBRA model fails to describe the inductance increase at lower frequencies, which is caused by the nonideal conductors and is, indeed, negligible for conventional MSLs (see Fig. 4). The principal characteristics are closely related to that of the CPW [10], [11]: In the skin-effect frequency range, L' increases with decreasing frequency due to the growing internal part. At lower frequencies then, the current distribution in the conductors, particularly the ground conductor, become more and more homogeneous. This causes changes in the magnetic-field distribution, which lead to a further increase in L'.

Regarding R' in Fig. 3, the LIBRA results coincide with the full-wave data only in the skin-effect range. The modified formulation proposed in this paper, on the other hand, fits the reference data with good accuracy. For $f \to 0$, the L' value of the full-wave analysis is somewhat larger than that of our model. The reason is that, for the mode-matching approach, magnetic sidewalls had to be assumed, whereas the solution for L'_{DC} in (16) refers to the structure without lateral boundaries, as depicted in Fig. 1.

Once the equivalent-circuit elements R', L', C', and G' are given, the propagation quantities, i.e., complex characteristic impedance Z_L^{ec}, attenuation α^{ec}, and effective relative dielectric constant $\varepsilon_{r,\mathrm{eff}}^{ec}$ can be easily determined. The superscript ec denotes the respect to the equivalent circuit

$$Z_L^{ec} = \sqrt{\frac{(R' + j\cdot\omega\cdot L')}{(G' + j\cdot\omega\cdot C')}} \tag{21}$$

$$\gamma^{ec} = \alpha^{ec} + j\beta^{ec} = \sqrt{(R' + j\cdot\omega\cdot L')\cdot(G' + j\cdot\omega\cdot C')} \tag{22}$$

$$\varepsilon_{r,\mathrm{eff}}^{ec} = \left(\frac{\beta^{ec}\cdot c_0}{\omega}\right)^2. \tag{23}$$

D. High-Frequency Dispersion

The closed-form approximations presented thus far rely on a quasi-TEM description. Therefore, the transverse characteristic dimensions such as signal conductor width w and substrate height h_s have to be small enough compared to the wavelength $\lambda = \lambda_0/\sqrt{\varepsilon_r}$ (usually, a limit of 1/10 is assumed). In order to expand the validity range of the new model to higher frequencies, dispersion formulas known from the literature are included. As a consequence, the new model can be used for TFMSLs, as well as for conventional MSLs.

Regarding dispersion of the effective relative dielectric constant, we refer to Kirschning and Jansen [5, p. 179], [6, p. 28], which yields

$$F\_\varepsilon = \frac{\varepsilon_{r,\mathrm{eff,dynamic}}}{\varepsilon_{r,\mathrm{eff,static}}} = \frac{\varepsilon_r}{\varepsilon_{r,\mathrm{eff},0}} - \left(\frac{\varepsilon_r}{\varepsilon_{r,\mathrm{eff},0}} - 1\right) \Big/ (1+P) \tag{24}$$

with $\varepsilon_{r,\mathrm{eff},0}$ according to (2) and

$$P = P1\cdot P2\cdot\left\{(0.1844 + P3\cdot P4)\cdot 10\cdot\frac{f\cdot h_s}{\mathrm{GHz\cdot cm}}\right\}^{1.5763}$$

$$P1 = 0.27488 + \left(\frac{w}{h_s}\right)\cdot\left[0.6315 + \frac{0.525}{\left(1 + 0.157\cdot\frac{f\cdot h_s}{\mathrm{GHz\cdot cm}}\right)^{20}}\right] - 0.065683\cdot\exp\left(-8.7513\cdot\frac{w}{h_s}\right)$$

$$P2 = 0.33622\cdot[1 - \exp(-0.03442\cdot\varepsilon_r)]$$

$$P3 = 0.0363\cdot\exp\left(-4.6\cdot\frac{w}{h_s}\right)\cdot\left\{1 - \exp\left[-\left(\frac{f\cdot h_s}{3.87\cdot\mathrm{GHz\cdot cm}}\right)^{4.97}\right]\right\}$$

$$P4 = 1 + 2.751\cdot\left\{1 - \exp\left[-\left(\frac{\varepsilon_r}{15.916}\right)^8\right]\right\}.$$

The term F_ε translates into a similar correction factor F_Z for characteristic impendance (see [6, p. 29])

$$F\_Z = \frac{Z_{L,\mathrm{dynamic}}}{Z_{L,\mathrm{static}}} = \frac{\varepsilon_{r,\mathrm{eff},0}\cdot F\_\varepsilon - 1}{\varepsilon_{r,\mathrm{eff},0} - 1}\cdot\frac{1}{\sqrt{F\_\varepsilon}}. \tag{25}$$

Using (24) and (25), the corresponding dispersion corrections for L' and C' can be derived as follows:

$$F\_L = F\_Z\cdot\sqrt{F\_\varepsilon} \tag{26}$$

$$F\_C = \frac{\sqrt{F\_\varepsilon}}{F\_Z}. \tag{27}$$

The dynamic values of L' and C' are calculated according to $L'_{\mathrm{dynamic}} = L'_{\mathrm{static}}\cdot F\_L$ and $C'_{\mathrm{dynamic}} = C'_{\mathrm{static}}\cdot F\_C$. For the static quantities, the expressions for L' and C' in (18) and (8) have to be inserted.

IV. Accuracy and Limitations

In developing the simplified description based on the cross section in Fig. 1, several assumptions had to be introduced which restrict the range of validity. These limitations are summarized in the following. First, it should be mentioned that the signal and ground conductor have the same thickness. Although the influence of this simplification is limited because signal conductor thickness dominates the behavior, this condition

is not always fulfilled in practice and could be the subject of future work.

Additional limitations for the model stem from the approximate formulas used, as there are

$$\frac{1}{2\pi} \le \frac{w}{h_s} \le \frac{1}{0.012}, \qquad 1 \le \varepsilon_r \le 20;\ t < w;$$
$$wg > w + 6 \cdot (h_s + t).$$

If these relations are violated, accuracy deteriorates.

Two further effects are to be discussed in this context, which are related to the ground conductor width and the influence of the substrate below the ground conductor:

Regarding ground-conductor width wg, one should note that wg has a strong influence on L' at low frequencies. It may cause changes of more than 100% in the dc limit. However, this effect can be neglected in the propagation quantities because, at low frequencies, one has $\omega \cdot L' \ll R'$ and the propagation constant $\gamma \approx \sqrt{j\omega \cdot R' \cdot C'}$ becomes almost independent of L'. The same arguments hold for the characteristic impedance. This applies, however, only to the dc limit for L', but not to the intermediate-frequency range (between f_0 and f_{sc}), where one needs an accurate description because $\omega \cdot L' \ll R'$ is not fulfilled there. Considering the line geometries of Figs. 3 and 4, for instance, the frequency with $R' = \omega \cdot L'$ is 6.6 GHz and, thus, located well within the intermediate range.

In most applications, the thin-film microstrip version is placed on top of a carrier substrate. The ground conductor of the TFMSL shields the transmission-line against the carrier substrate. For nonideal conductors, this shielding effect vanishes if the skin depth δ becomes large compared to metallization thickness t. Following quasi-TEM theory, this affects only the magnetic field and, consequently, line inductance L' and the resistance R' of the ground conductor. The transverse electric field, on the other hand, is determined by electrostatics. Thus, capacitance C' and conductance G' remain unchanged as far as the conductivity of the ground metal is nonzero. One concludes that the conductivity of the carrier substrate may have an influence on L' and R' at low frequencies, i.e., for $\delta \gg t$. In this case, a part of the ground current flows within the carrier substrate, which causes small changes of R' and L' at low frequencies (around f_0). This effect can be neglected, however, if conductivity of the carrier substrate is considerably lower than that of the ground metallization.

In order to check accuracy of the new model, we compared the resulting propagation quantities with full-wave simulation data [7]. An example is shown in Figs. 5–7. Additionally, the results of the microstrip model used in Libra or ADS from HP-EEsof are included for comparison. A more systematic investigation considering various common TFMSL structures (with $w = 8, \ldots, 140$ μm, $h_s = 1.7, \ldots, 50$ μm, $t = 0.8, \ldots, 3.5$ μm) yields the following deviations:

$$\left|\frac{\Delta\beta}{\beta}\right| < 2\%, \quad \left|\frac{\Delta Z_L}{Z_L}\right| < 3\%, \quad \left|\frac{\Delta\alpha}{\alpha}\right| < 8\%.$$

The largest deviations occur in the intermediate-frequency region between dc and skin-effect range, where purely approximate formulas describe the R' and L' behavior. Overall, however, the accuracy is sufficient for application of the TFMSL model in practical circuit design.

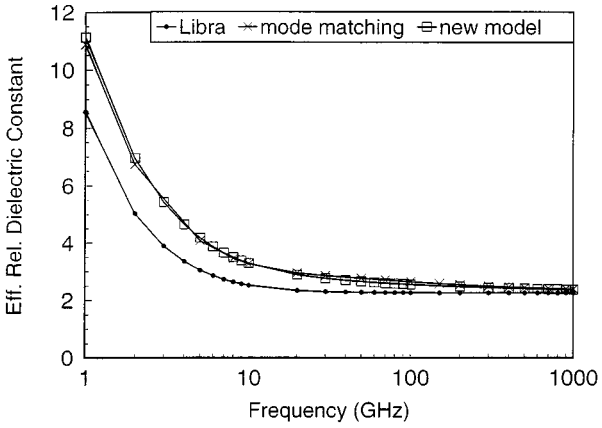

Fig. 5. Effective relative dielectric constant as a function of frequency: comparison of new model with results of full-wave simulations ([7]) and Libra (for TFMSL data see Fig. 3).

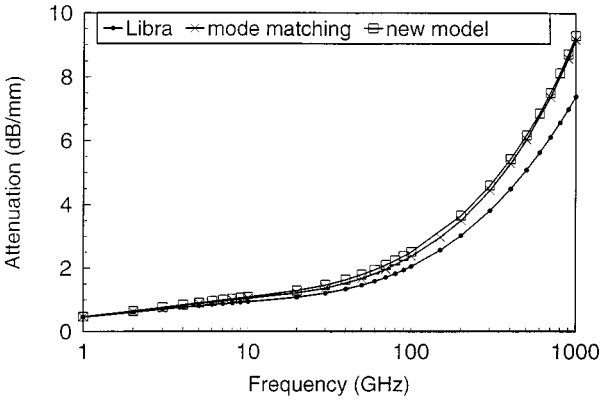

Fig. 6. Attenuation against frequency (other data as in Fig. 3).

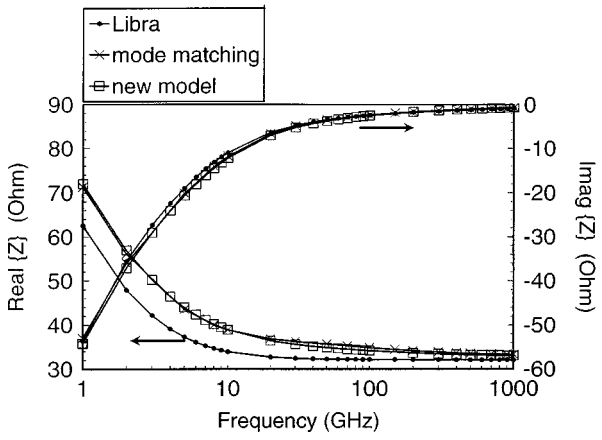

Fig. 7. Characteristic impedance (real and imaginary part) as a function of frequency (other data as in Fig. 3).

V. Conclusions

- Modeling of the TFMSL requires modifications of the conventional microstrip tools available in a variety of software packages. This is a consequence of the difference in

transverse dimensions, particularly the fact that the ratio t/h_s between strip thickness t and substrate height h_s is much larger than for standard microstrips.

- What is necessary for the TFMSL is a more detailed description of nonideal conductivity and finite metallization thickness, which influences line inductance and resistance.
- Taking these effects into consideration, an extended microstrip model is presented, which includes the TFMSL case, but of course, holds for conventional microstrip structures as well. The model uses closed-form expressions and can be easily implemented in common software tools. The frequency range of validity extends down to dc. For typical TFMSL dimensions, the upper limit reaches well into the submillimeter-wave range.

REFERENCES

[1] M. Case, S. Maas, L. Larson, D. Rensch, D. Harame, and B. Meyerson, "An X-band monolithic active mixer in SiGe HBT technology," in *IEEE MTT-S Int. Microwave Symp. Dig.*, vol. 2, 1996, pp. 655–658.

[2] I. Toyoda, K. Nishikawa, T. Tokumitsu, K. Kamogawa, C. Yamaguchi, M. Hirano, and M. Aikawa, "Three-dimensional masterslice MMIC on Si substrate," *IEEE Trans. Microwave Theory Tech.*, vol. 45, pp. 2524–2530, Dec. 1997.

[3] J. Wolf, F. J. Schmückle, W. Heinrich, M. Töpper, K. Buschick, O. Ehrmann, and H. Reichl, "System integration for high frequency wireless applications," in *Proc. 3rd Annu. Wireless Commun. Conf.*, San Diego, CA, Nov. 1–2, 1998, pp. 37–46.

[4] H.-M. Heiliger, M. Nagel, H. G. Roskos, H. Kurz, F. Schnieder, and W. Heinrich, "Thin-film microstrip lines for mm and sub-mm-wave on-chip interconnects," in *IEEE MTT-S Int. Microwave Symp. Dig.*, 1997, pp. 421–424.

[5] R. K. Hoffmann, *Integrierte Mikrowellenschaltungen*. Berlin, Germany: Springer-Verlag, 1983.

[6] K. C. Gupta, R. Garg, and I. Bahl, *Microstrip Lines and Slot Lines*, 2nd ed. Norwood, MA: Artech House, 1996.

[7] W. Heinrich, "Full-wave analysis of conductor losses on MMIC transmission lines," *IEEE Trans. Microwave Theory Tech.*, vol. 38, pp. 1468–1472, Oct. 1990.

[8] E. Hammerstad and O. Jensen, "Accurate models for microstrip computer-aided design," in *IEEE MTT-S Int. Microwave Symp. Dig.*, 1980, pp. 407–409.

[9] A. R. Djordjevic and T. K. Sarkar, "Closed-form formulas for frequency-dependent resistance and inductance per unit length of microstrip and strip transmission lines," *IEEE Trans. Microwave Theory Tech.*, vol. 42, pp. 241–248, Feb. 1994.

[10] H. Klingbeil and W. Heinrich, "Calculation of CPW AC resistance and inductance using a quasi-static mode-matching approach," *IEEE Trans. Microwave Theory Tech*, vol. 42, pp. 1004–1007, June 1994.

[11] W. Heinrich, "Quasi-TEM description of MMIC coplanar lines including conductor loss effects," *IEEE Trans. Microwave Theory Tech.*, vol. 41, pp. 45–52, Jan. 1993.

Frank Schnieder was born in Ludwigsfelde, Germany, in 1960. He received the Dipl.-Ing. and Dr.-Ing. degrees in electrical engineering from the Technical University of Dresden, Dresden, Germany, in 1986 and 1990, respectively.

Since 1989, he has been involved with GaAs MMICs. In 1992, he joined the Ferdinand-Braun-Institut für Höchstfrequenztechnik, Berlin, Germany. His current research is focused on MMIC design and transmission-line modeling.

Wolfgang Heinrich (M'84–SM'95) was born in Frankfurt/Main, Germany, in 1958. He received the Dipl.-Ing., Dr.-Ing., and the habilitation degrees from the Technical University of Darmstadt, Darmstadt, Germany, in 1982, 1987 and 1992, respectively.

In 1983, he joined the staff of the Institut für Hochfrequenz-Technik, Technical University of Darmstadt, where he was involved with field-theoretical analysis and simulation of planar transmission lines. Since April 1993, he has been with the Ferdinand-Braun-Institut für Höchstfrequenztechnik, Berlin, Germany, where he is Head of the Microwave Department. His current research activities focus on MMIC modeling, coplanar circuit design, and related packaging issues.